Multivariate mediation analysis with voxel-based morphometry revealed the neurodegeneration pathways from genetic variants to Alzheimer's Disease

Shizhuo Mu, MS[1], Jingxuan Bao, MA[1], Hanxiang Xu, BS[1], Manu Shivakumar, MS[1], Shu Yang, PhD[1], Xia Ning, PhD[2], Dokyoon Kim, PhD[1], Christos Davatzikos, PhD[1], Haochang Shou, PhD[1], Li Shen, PhD[1], for the ADNI
[1]University of Pennsylvania, Philadelphia, PA 19104, USA; [2]The Ohio State University, Columbus, OH 43210, USA

Abstract

Neurodegenerative processes are increasingly recognized as potential causative factors in Alzheimer's disease (AD) pathogenesis. While many studies have leveraged mediation analysis models to elucidate the underlying mechanisms linking genetic variants to AD diagnostic outcomes, the majority have predominantly focused on regional brain measure as a mediator, thereby compromising the granularity of the imaging data. In our investigation, using the imaging genetics data from a landmark AD cohort, we contrasted both region-based and voxel-based brain measurements as imaging endophenotypes, and examined their roles in mediating genetic effects on AD outcomes. Our findings underscored that using voxel-based morphometry offers enhanced statistical power. Moreover, we delineated specific mediation pathways between SNP, brain volume, and AD outcomes, shedding light on the intricate relationship among these variables.

Introduction

Alzheimer's Disease (AD) is a progressive neurodegenerative disorder with high estimated heritability [1, 2, 3, 4, 5]. It is characterized by the presence of prominent amnestic cognitive impairment, where the degree of cognitive impairment in AD has demonstrated a significant effect on the patient's desires and abilities to engage in daily activities [6]. Moreover, the effect of AD is broad and far-reaching, affecting more than 6% of the elder population worldwide [7] and imposes a high economic and socio-psychological burden.

Despite the considerable impact of AD and numerous efforts to understand its underlying mechanisms, the precise cause of AD remains elusive. Within the AD research community, identifying therapeutic targets has been a long-standing focus, particularly through the exploration of genetic pathways related to the disease. Numerous studies have investigated the connection between genetic variants and AD diagnosis using genome-wide association study (GWAS) methods. For example, Bellenguez et al. identified 75 risk loci associated with AD, which were further analyzed through pathway enrichment and gene prioritization [8]. While these studies have advanced our understanding of the genetics of AD, there is still room for improvement in unraveling the complexities of its pathology.

To understand the AD pathogenesis, researchers have developed various hypotheses of AD [9, 10]. Among those, neurodegeneration is considered to be one of the major pathways of AD, as the gradual loss of neurons and their connections accounts for the cognitive decline and behavioral alterations observed in patients. With the advancement of medical imaging technology, magnetic resonance imaging (MRI) has made it possible to image the brain, capturing the brain structure and offering invaluable insights into the study of neurodegenerative processes.

Many studies explored the role of the neurodegeneration in AD. For instance, Bao et al. established a putative AD causal pathway from a systems biology perspective: the SNP rs6585827 mutation upregulates the expression of the *BTBD16* gene in oligodendrocytes, which in turn lessens the risk of volume loss in the entorhinal cortex, thereby exerting a protective effect against AD [11]. Another study by Wen et al. identified two dominant dimensions of brain atrophy in patients with symptomatic mild cognitive impairment (MCI) and AD - the "diffuse-AD" dimension showing widespread brain atrophy, and the "MTL-AD" dimension displaying focal medial temporal lobe atrophy. These dimensions were found to be associated with distinct pathological mechanisms, including cardiovascular diseases, inflammation, and hormonal dysfunction [12]. However, they were using regional brain volume as their quantitative indicator for the brain, which may overlook the intrinsic inter-relationship between brain voxels within brain regions. This limitation could lead to a loss of critical information and diminished statistical power in the analyses.

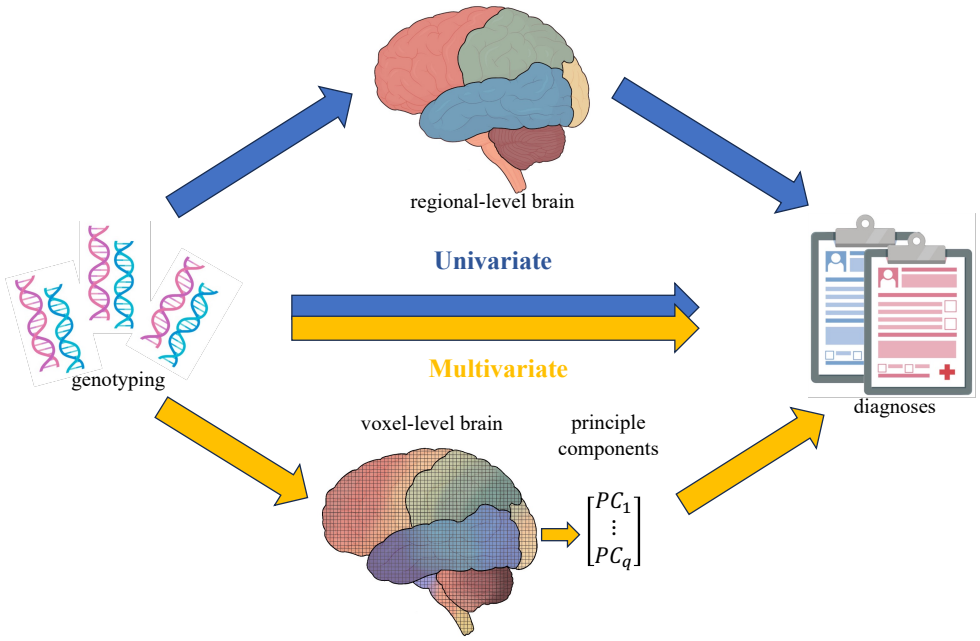

Figure 1: Workflow used in this study. In univariate mediation analysis, feature of each region was represented by the mean value of voxel-level volumetric measures. In multivariate mediation analysis, unrelated principle components of voxel-level measures in each region were first calculated to reduce dimension.

To bridge this gap, we conducted genetics-imaging-diagnosis mediation analyses to explore the role of brain volume as a mediator between genetic variants and AD outcomes. In our present study, we intensively examined the associations between genetics and AD that are significantly mediated by variations in brain morphometry. We carried out an extensive comparison between region-based and voxel-based analyses with the aim of providing robust evidence that voxel-based brain morphometric measures can enhance the quality and precision of the analysis.

Methods

To explore how regional brain morphometry mediates the relationship between genetics and AD, we conducted a comprehensive mediation analysis. Specifically, our analysis focuses on identifying imaging-derived endophenotypes [13] that can mediate these genetic associations with AD. To assess the impact of different imaging resolutions on mediation discovery, we compared the mediation signals derived from both univariate and multivariate mediation analyses. In our study, we treated imputed genotyping data as the exposure variable, regional brain morphometry as the mediator, and AD diagnostic case-control phenotype as the outcome variable. In the univariate mediation analysis, we used regional brain morphometry as the sole mediator. Meanwhile, in the multivariate mediation analysis, we considered the voxel-level brain morphometry measures within each region as a group of mediators. This dual approach aimed to offer a more nuanced understanding of the complex relationships between genetic factors, brain structure, and AD outcomes (Figure 1).

Univariate Mediation Analysis For the univariate mediation analysis, we calculated the mean value of the voxel-level measures as the mediator for each brain region. Then we followed VanderWeele's guide [14] to perform mediation analysis for identifying this regional volumetric measure as potential disease mediators.

Let $Y \in \{0, 1\}$ denote the dependent variable. In our study, Y represents the AD case-control phenotype (0:control, 1:case). Let X denote the independent exposure variable, which is one of the 57 AD-related single nucleotide polymorphisms (SNPs). Let Z be the covariates which include age, sex, and 10 principle components (PCs) of population

structure that can capture population structure, and M be one region of the brain imaging mediators.

Our mediators, regional brain morphometry measures, are believed to obey normal distribution, while our outcome is a binary variable indicating whether or not the subjects were diagnosed as AD patients. Plus, 39.8%, 62.7%, 28.3%, and 70.0% are cases within 4 comparison groups, which turned out that the outcome is not rare (10% is often used as a cutoff as VanderWeele discussed [14]). Thus, instead of standard logistic regression, we choose log binomial regression model.

Step 1: We use linear regression model to fit the imaging mediator M against the SNP value X, controlling for Z:

$$M = \beta_{21}X + \beta_{22}Z + \epsilon_2, \tag{1}$$

where the coefficient β_{21} should be significant (adjusted p-value < 0.05) after correcting for multiple comparisons (We employ Bonferroni correction) to pass the first step.

Step 2: We use log-binomial regression model to fit the diagnostic outcome Y against both the SNP value X and mediator M, controlling for Z:

$$log\{P_r(Y = 1|X, M, Z)\} = \beta_{11}X + \beta_{12}M + \beta_{13}Z + \epsilon_1, \tag{2}$$

where the coefficient β_{11} should be significant (adjusted p-value < 0.05) after correcting for multiple comparisons (We employ Bonferroni correction) to pass the second step.

Step 3: If the test passed the first and the second step, we can use the product method to conclude the direct effect (DE) and the indirect effect (IE) for its pathway:

$$DE = \beta_{11}, \tag{3}$$

$$IE = \beta_{21}\beta_{12}, \tag{4}$$

Multivariate Mediation Analysis For the multivariate mediation analysis, we drew inspiration from the methodology outlined by Yen Tsung Huang et al. [15]. In contrast to the univariate approach, we utilized voxel-based information from the brain imaging data, leading to a high-dimensional mediator. To deal with the high dimensionality issue, we first calculated principle components of voxelwise measures in each brain region, and then employed these principle components as mediators for mediation analysis.

Similar with univariate case, for subject j, let $Y \in \{0, 1\}$ be the outcome; $\mathbf{Z}$ be the covariates including sex, age, and the 10 PCs. Let $X \in \{0, 1, 2\}$ denote the exposure single variant, and $\mathbf{M}$ denote the multivariate mediator including multiple voxels within a brain region. Thus, our multivariate mediation analysis included two steps:

Step 1: To reduce the dimension of mediators, we transformed the correlated voxel level mediators in the same brain region to be uncorrelated elements $\mathbf{P}$. The new mediator $\mathbf{P}$ can explain 80% variance.

$$\mathbf{P} = \mathbf{uM}, \tag{5}$$

where u is an orthogonal matrix that makes $\mathbf{u\Sigma u}^T = diag(\sigma_1^2, ..., \sigma_q^2)$ and $\sigma_1^2 > ... > \sigma_q^2$ hold. $\mathbf{\Sigma}$ is the $q \times q$ covariance matrix for q elements within a multivariate mediator.

Step 2: We used the transformed uncorrelated mediator elements to fit the two regression models in the mediation analysis. Let $\mathbf{P} = \{P_1, ..., P_p\}$, then for each element P_i inside the $\mathbf{P}$, both two regression models should be fitted.

$$log\{P_r(Y = 1|X, P_i, Z)\} = \gamma_i X + \beta_i P_i + \boldsymbol{\eta_i Z} + \epsilon_3, \tag{6}$$

$$P_i = \alpha_i X + \boldsymbol{\delta}_i \mathbf{Z} + \epsilon_4. \tag{7}$$

After the estimates of each element within a brain region were calculated, we can obtain the indirect effect and combined p-value of this region:

$$IE_{multi} = \sum_{i}^{p} \alpha_i \beta_i \tag{8}$$

$$p - value = 2 * \left\{ 1 - \Phi\left(\frac{IE_{multi}}{\sigma_{simIE}} \right) \right\} \tag{9}$$

where σ_{simIE} is the standard deviation of the simulated total indirect effects across all bootstrap simulations.

Materials

The demographic, genotyping, and imaging data used in the preparation of mediation analysis were obtained from the Alzheimer's Disease Neuroimaging Initiative (ADNI) database (http://adni.loni.usc.edu) [16, 17]. The ADNI was launched in 2003 as a public-private partnership, led by Principal Investigator Michael W. Weiner, MD. The primary goal of ADNI has been to test whether serial magnetic resonance imaging (MRI), positron emission tomography (PET), other biological markers, and clinical and neuropsychological assessment can be combined to measure the progression of mild cognitive impairment (MCI) and early Alzheimer's disease (AD). Up-to-date information about the ADNI is available at www.adni-info.org.

We used genotyping data from ADNI 1, GO, 2, and 3 studies [18, 19, 20]. In our study, McCarthy Group Tools (https://www.well.ox.ac.uk/~wrayner/tools/) were used for alignment. We aligned the genotyping data to the Homo sapiens (human) genome assembly NCBI37 (hg19) genome builder, according to 1000 Genome phase 3 [21]. To complement the missing data, we imputed thoes genotypes using the Michigan Imputation Server [22] with 1000 Genome phase 3 reference panel of European ancestry. We annotated our imputed genotyping data using ANNOVAR [23]. After alignment and imputation, we performed the quality control (QC) using the following criteria: genotyping call rate $> 98\%$, minor allele frequency $> 0.1\%$, Hardy-Weinberg Equilibrium $>$ 1e-6, missingness per individual $< 5\%$. After QC, our data were obtained by additive recoding the minor alleles per person. All the QC and recoding were performed using PLINK 1.9 [24].

T1-weighted MRI data were chosen as our mediators. These imaging data were downloaded from the ADNI 1, GO, 2, and 3 studies [16, 17]. Raw 3D T1-weighted MRIs were first quality checked for motion, image artifacts, or restricted field-of-view. Another QC was performed as follows: first, the images were examined by manually evaluating for pipeline failures (e.g., poor brain extraction, tissue segmentation, and registration errors). Furthermore, a second-step automated procedure automatically flagged images based on outlying values of quantified metrics (i.e., ROI values), and those flagged images were re-evaluated. The quality-controlled images are first corrected for magnetic field intensity inhomogeneity [25]. Voxel-wise regional volumetric maps (RAVENS) for each tissue volume [26] are generated by spatially aligning the skull-stripped images to a template residing in the MNI-space [27]. A multi-atlas parcellation method (MUSE) [28] was then used to extract 139 regions of interest (ROIs) from gray matter and white matter tissue maps. After data preprocessing, we matched the common subjects with genotyping, imaging, and demographic data. After matching, there are 1,534 subjects left with main characteristics summarized in Table 1.

For the genotypes, we have ordinal data with the values of 0, 1, and 2, where 0 represents the base pair at corresponding genome location has homozygous reference alleles, 1 represents a heterozygous variant, and 2 represents a homozygous genetic variant. For the brain imaging mediators, we used the RAVENS measurement as our mediators, which can be intuitively explained as the brain volumetric variations. We assume that the measurement follows a normal distribution. The outcome is a binary variable indicating whether or not the subjects were diagnosed as AD patients.

Table 1: Subjects characteristics in this study. P-values were calculated to examine whether the differences among different groups are significant. P-value for gender was calculated with χ^2 test, and p-value for age was calculated with one-way ANOVA. HC = Healthy Control; MCI = Mild Cognitive Impairment; AD = Alzheimer's Disease.

Diagnosis	HC	MCI	AD	p-value
Number	447	750	296	-
Gender(M/F)	229/218	457/293	163/133	**2.2E-16**
Age(mean $\pm$ sd)	74.33 $\pm$ 5.65	73.05 $\pm$ 7.63	74.88 $\pm$ 7.81	0.211

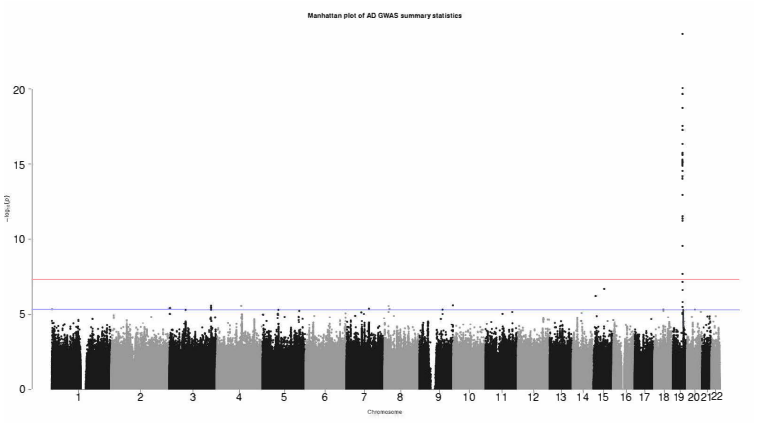

Figure 2: Manhattan plot of AD GWAS summary statistics. The blue line shows the threshold of 5e-6, which is our selection threshold. The red line indicates 5e-8 threshold.

For the univariate mediation analysis, despite varying voxel counts within each brain region, we opted to compute the mean value across these voxels to represent the region and reduced the dimensionality. As a result, in the univariate study, each mediator is represented by a single value.

Results

Genome wide association study on AD In mediation analysis, a significant mediation association relationship requires two conditions: 1) Significant total effect: The genetic variants (exposure) and AD case-control diagnostic outcome (outcome) should have a significant association relationship; and 2) Significant indirect effect: The regional brain volumetric phenotype (mediator) should significantly mediate the association relationship between genetic variants (exposure) and AD case-control diagnostic outcome (outcome).

In our framework, we first performed a GWAS on the AD case-control diagnostic outcome to screen for the genetic variants that have significant association relationship with AD. Intuitively, the GWAS screening will prioritize those exposure-outcome pairs with significant total effects. Specifically, we fit a logistic regression model treating the AD case-control phenotype as dependent variable and the genetic variants as independent variables. To control for the other unrelated confounding variables, we adjusted the logistic regression model using age, sex, and population structure characterized by the first ten principal components derived from linkage disequilibrium (LD) pruned genotyping data. These confounding variables are all widely studied and shown to be significantly associated with AD progression. Our GWAS was performed using PLINK2[1] [29].

In our AD case-control GWAS analysis of 18,366,758 SNPs, we prioritized 57 SNPs that passed a suggestive genome-wide significant threshold of 5e-6 (Figure 2). Among prioritized 57 SNPs, 38 of them are located in chromosome 19. We further mapped the prioritized SNPs to their closest gene using ANNOVAR[2] [23], and the results highlighted

[1]https://www.cog-genomics.org/plink/2.0/
[2]https://annovar.openbioinformatics.org/en/latest/

Table 2: Top 5 results of univariate mediation results. Here we present original uncorrected p-values to indicate their ranks more clearly. After bonferroni correction, these results are all insignificant. PCgG: posterior cingulate gyrus; BF: basal forebrain; AOrG: anterior orbital gyrus; MOrG: medial orbital gyrus; PT: planum temporale; MPoG: medial postcentral gyrus; TTG: transverse temporal gyrus; ITG: inferior temporal gyrus; FuG: fusiform gyrus; CE: cerebellum exterior.

HC vs MCI+AD			**HC vs MCI**		
SNP	Region	p-value	SNP	Region	p-value
4:105589137	Left PCgG	0.012	9:96604808	Right MPoG	0.024
9:96604808	Left BF	0.012	19:45428234	Left MPoG	0.038
4:105589137	Left AOrG	0.016	19:45388130	Left MPoG	0.044
9:96604808	Left MOrG	0.020	19:45422160	Left MPoG	0.048
4:105589137	Right PT	0.022	19:45428234	Right MPoG	0.052
HC vs AD			**MCI vs AD**		
SNP	Region	p-value	SNP	Region	p-value
19:45409167	Left Amygdala	0.216	19:45395266	Right ITG	0.118
8:20832164	Left TTG	0.286	19:45395266	Right FuG	0.118
9:96604808	Left Amygdala	0.298	19:45410002	Right MPoG	0.120
8:20832307	Left TTG	0.318	19:45413224	Right FuG	0.134
8:20832214	Left TTG	0.322	19:45395266	Right CE	0.136

NECTIN2, *TOMM40*, *APOE*, and *APOC1* genes. This discovery aligns with the majority of AD GWAS studies, which reassures the validity of our GWAS findings.

Voxel-based imaging measures can capture more intrinsic association In our study, we aim to examine the mediated associations between genetic variants and AD diagnosis through regional brain morphometry, as well as to compare the statistical power between univariate and multivariate mediation methods. We consider each genetic variant as an exposure, each imaging-derived endophenotype extracted from structural brain MRI as a mediator, and the case-control AD diagnosis as an outcome. GWAS with PLINK2 has helped us prioritize 57 SNPs for further study. Our next analysis encompasses a comparison of mediation effects across the 57 prioritized genetic variants and 139 brain regions of interest, leading to, in total, 7,923 mediation experiments. For each of these analyses, we conducted both univariate and multivariate mediation analyses. We divided the subjects into four groups for comparisons - healthy control subjects vs AD patients (HC vs AD), healthy control subjects vs patients with MCI (HC vs MCI), MCI patients vs AD patients (MCI vs AD), and healthy control subjects vs MCI+AD patients (HC vs MCI+AD). For both univariate and multivariate mediation analyses, the case-control phenotype for four different groups were used as outcomes. In the univariate analysis, we treated the regional brain morphometry as a single feature. Conversely, in the multivariate analysis, we consider all the voxel-level brain morphometry within the corresponding brain region as mediators. In our study, we reported the SNP-ROI pairs with the p-value for the indirect effect less than 0.05 after Bonferroni correction, of which we call "significant mediation effect".

Multivariate mediation analysis identified stronger signals, which indicated that we could capture more information from voxel-based brain morphometry. For the univariate mediation analyses, we found no significant mediation effects in any of the four groups. Top 5 signals of univariate cases are listed in Table 2.

In contrast, for the multivariate mediation analyses where we treat all the voxels within a brain region as mediators, we discovered 1,702 significant regional brain morphometry mediated SNP-AD associations in HC vs MCI+AD group. Herein, we use partial mediation effect to represent all total effect, indirect effect, and direct effect are significant. Full effect means that only total effect and indirect effect are significant. As a result, all of the 1,702 signals have partial mediation effects. Eighty significant mediating pairs were identified in HC vs AD group, comprising 15 with partial effects and 65 with full effects. Fifty-seven significant pairs were identified in MCI vs AD group, with all 57 signals displaying full effects. And 23 significant pairs were identified in HC vs MCI group, with 3 demonstrating partial effects and 20 showing full effects (Figure 3).

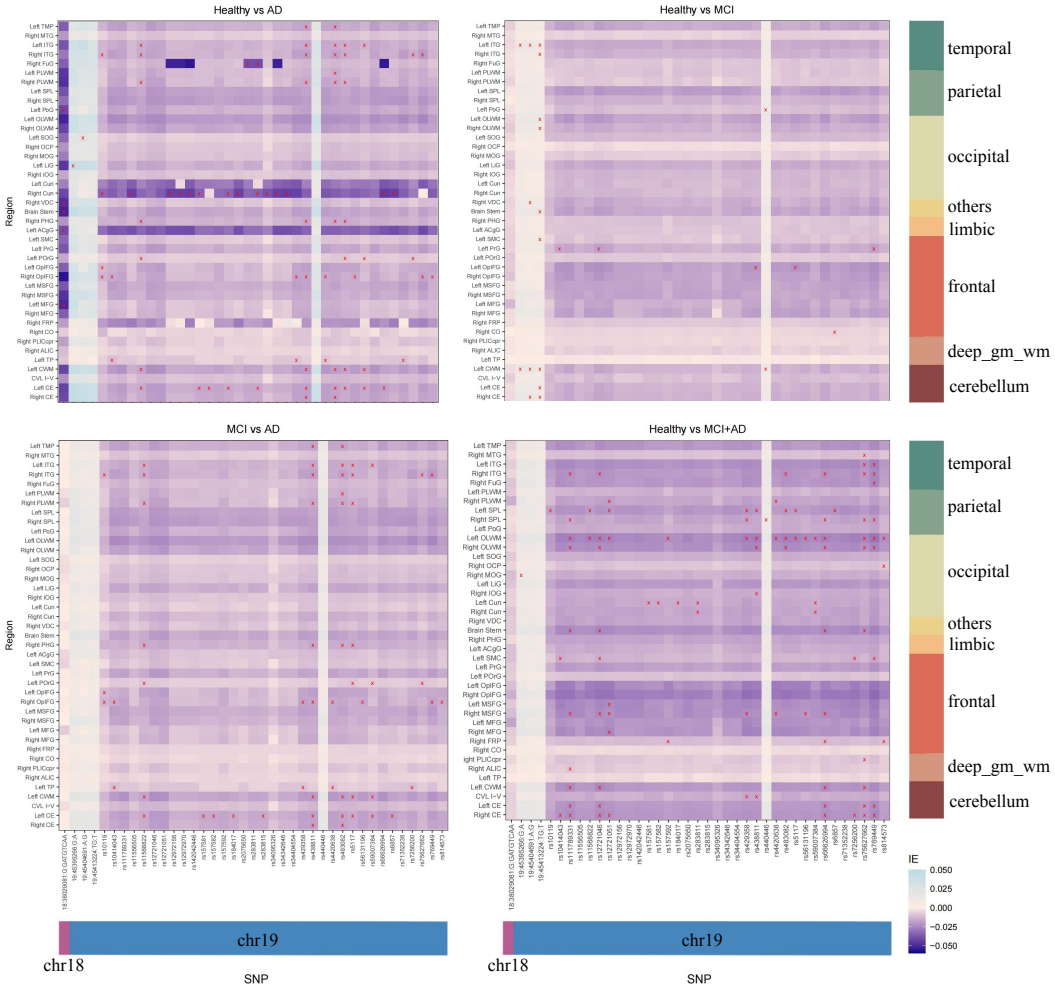

Figure 3: Heatmaps of indirect effect sizes of multivariate mediation among different four comparison groups. The healthy vs MCI+AD group only shows top 100 signals. The color bar on the right indicates brain region groups, while the color bar on the bottom shows different chromosomes. The red cross means that this SNP-ROI pair significantly mediated the SNP-AD associations. For the brevity, abbreviations have been used for brain regions: TMP: temporal pole; MTG: middle temporal gyrus; ITG: inferior temporal gyrus; FuG; fusiform gyrus; PLWM: parietal lobe whigt matter; SPL: superior parietal lobule; PoG: postcentral gyrus; OLWM: occipital lobe white matter; SOG: superior occipital gyrus; OCP: occipital pole; MOG: middle occipital gyrus; LiG: lingual gyrus; IOG: inferior occipital gyrus; Cun: cuneus; VDC: ventral dorsal cortex; PHG: parahippocampal gyrus; ACgG: anterior cingulate gyrus; SMC: supplementary motor cortex; PrG: precentral gyrus; POrG: posterior orbital gyrus; OpIFG: opercular part of the inferior frontal gyrus; MSFG: superior frontal gyrus medial segment; MFG: middle frontal gyrus; FRP: frontal pole; CO: central operculum; PLICcpr: posterior limb of internal capsule incuding cerebral peducle; ALIC: anterior limb of internal capsule; TP: thalamus proper; CWM: cerebellar white matter; CVL: cerebellar vermal lobules; CE: cerebellum exterior; deep_gm_wm: deep structure of gray matter and white matter.

From our analysis, we are able to observe a clear decrease in terms of number of significant mediation effects derived from CN vs MCI+AD group compared to the other three comparison groups. This might be due to the significant difference with respect to the sample size: larger sample size could yield a stronger statistical power to detect the mediation signal. More interestingly, we also discovered that the number of significant mediation effects shows a decreased pattern when comparing the CN vs AD group, the MCI vs AD group, and the CN vs MCI group. Given

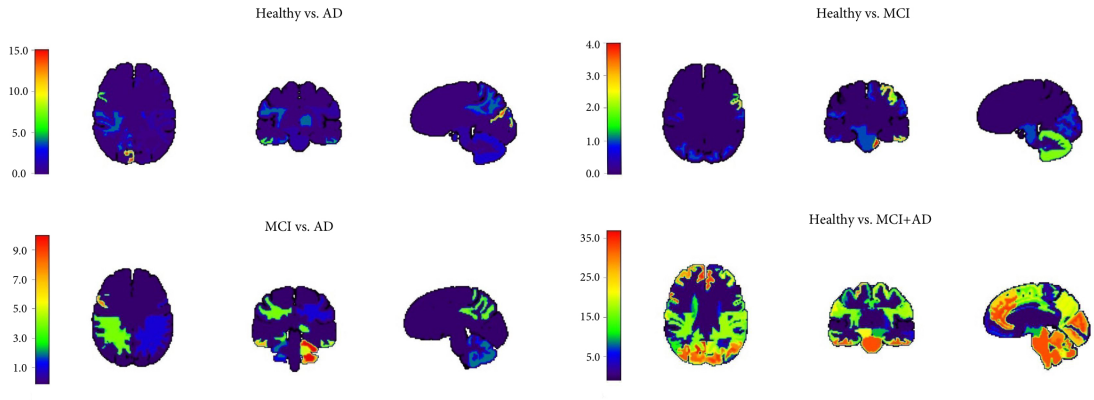

Figure 4: Brain Map. The color indicates the number of SNPs mediated by each region.

that the difference of the sample sizes in these three comparison groups are moderate, such decreasing pattern is more likely to lead us to the conclusion that MCI patients are genetically more similar to the cognitively normal subjects than to the AD patients.

In our multivariate mediation analysis, we found 86 brain regions having at least one significant mediation effect on the SNP-AD associations where 43 SNPs have at least one significant mediation effect. Specifically, the right cuneus has the most significant mediation signals in HC vs AD group - 14 SNP-AD associations are significantly mediated. Left CE has the most significant mediation signals in MCI vs AD group - mediating 10 SNP-AD associations. Left CWM has the most significant signals in HC vs MCI group - mediating 4 SNP-AD pairs. Left SPL has the most significant signals in HC vs MCI+AD group - 38 SNPs are mediated through this region. Our mediation results can be supported by substantial evidence. For example, right cuneus is located in the the occipital lobe of the brain and is believed to be significantly associated with the function of basic visual processing. A previous study showed that the right cuneus plays a significant role in the early AD pathology: AD patients excibit a significant volumetric reduction in the right cuneus [30]. Another study indicates a significant greater amount of senile plaques and neurofibrillary tangles were observed within the group of AD patients in the cuneus region than in the other regions that primarily controls the subjects' visual function [31]. Corriveau verified that the left SPL exhibited different activation patterns in relation to AD progression stages[32]. Our study further pinpoints the genetic underpinnings of the loss of visual functions in the AD patients and reveals a putative AD pathology: rs10119, rs11556505, rs12972156, rs12972970, rs142042446 etc. genetic variants within intronic *NECTIN2*, *APOE*, and *TOMM40* and upstream *TOMM40* can contribute to the volume loss in the right cuneus region, leading to both the impaired visual function and AD progression.

Conclusion

In this study, we investigated the mediation pathways of neurodegeneration in SNP-AD associations and accessed the gap of statistical power of univariate and multivariate mediation analyses. Our framework began with the prioritization of SNP variants through an AD GWAS. Then, we subsequently conducted both univariate and multivariate mediation

Table 3: Comparison between different groups.

(group 1) vs (group 2)	common SNPs	common regions
(HC vs MCI+AD) vs (HC vs AD)	31	21
(HC vs MCI+AD) vs (MCI vs AD)	19	12
(HC vs MCI+AD) vs (HC vs MCI)	10	13
(HC vs AD) vs (MCI vs AD)	19	13
(HC vs AD) vs (HC vs MCI)	19	9
(MCI vs AD) vs (HC vs MCI)	5	6

analysis using the prioritized genetic markers. Specifically, for each SNP variant and each brain region of interest, we used the regional brain morphometry as a single mediator in the univariate mediation analysis whereas we treat all the voxel-level measurements within the corresponding brain region as a group of mediators in the multivariate scenario. Our results reveal that multivariate mediation analysis can significantly empower the AD research compared to the univariate case. This might be due to the fact that multivariate mediation model is designed to capture the intrinsic inter-relationship between brain voxels. As a result, we identified potential neurodegeneration pathways, providing guidance for further experiments. For example, genetic variants within the intronic *NECTIN2*, *APOE*, and *TOMM40* and upstream *TOMM40* can contribute to the volume loss in the right cuneus region, leading to both the impaired visual function and AD progression. However, our study was potentially restricted by limited sample size. In future research, we plan to incorporate data from the UK Biobank, involving a larger number of subjects for enhanced statistical power.

Acknowledgments This work was supported in part by National Institutes of Health grants U01 AG068057, U01 AG066833, R01 AG071470, and RF1 AG068191. Data collection and sharing for this project was funded by the Alzheimer's Disease Neuroimaging Initiative (ADNI) (National Institutes of Health Grant U01 AG024904) and DOD ADNI (Department of Defense award number W81XWH-12-2-0012). ADNI is funded by the National Institute on Aging, the National Institute of Biomedical Imaging and Bioengineering, and through generous contributions from the following: AbbVie, Alzheimer's Association; Alzheimer's Drug Discovery Foundation; Araclon Biotech; BioClinica, Inc.; Biogen; Bristol-Myers Squibb Company; CereSpir, Inc.; Cogstate; Eisai Inc.; Elan Pharmaceuticals, Inc.; Eli Lilly and Company; EuroImmun; F. Hoffmann-La Roche Ltd and its affiliated company Genentech, Inc.; Fujirebio; GE Healthcare; IXICO Ltd.; Janssen Alzheimer Immunotherapy Research & Development, LLC.; Johnson & Johnson Pharmaceutical Research & Development LLC.; Lumosity; Lundbeck; Merck & Co., Inc.; Meso Scale Diagnostics, LLC.; NeuroRx Research; Neurotrack Technologies; Novartis Pharmaceuticals Corporation; Pfizer Inc.; Piramal Imaging; Servier; Takeda Pharmaceutical Company; and Transition Therapeutics. The Canadian Institutes of Health Research is providing funds to support ADNI clinical sites in Canada. Private sector contributions are facilitated by the Foundation for the National Institutes of Health (www.fnih.org). The grantee organization is the Northern California Institute for Research and Education, and the study is coordinated by the Alzheimer's Therapeutic Research Institute at the University of Southern California. ADNI data are disseminated by the Laboratory for Neuro Imaging at the University of Southern California.

Reference

1. Bao J, Wen Z, Kim M, Zhao X, Lee BN, Jung SH, et al. Identifying highly heritable brain amyloid phenotypes through mining Alzheimer's imaging and sequencing biobank data. In: PACIFIC SYMPOSIUM ON BIOCOMPUTING 2022. World Scientific; 2021. p. 109-20.
2. Gatz M, et al. Role of Genes and Environments for Explaining Alzheimer Disease. Archives of General Psychiatry. 2006 02;63(2):168-74. Available from: https://doi.org/10.1001/archpsyc.63.2.168.
3. Wingo TS, Lah JJ, Levey AI, Cutler DJ. Autosomal Recessive Causes Likely in Early-Onset Alzheimer Disease. Archives of Neurology. 2012 01;69(1):59-64. Available from: https://doi.org/10.1001/archneurol.2011.221.
4. Sims R, Hill M, Williams J. The multiplex model of the genetics of Alzheimer's disease. Nature Neuroscience. 2020 Mar;23(3):311-22. Available from: https://doi.org/10.1038/s41593-020-0599-5.
5. Wan J, Zhang Z, Rao BD, Fang S, Yan J, Saykin AJ, et al. Identifying the neuroanatomical basis of cognitive impairment in Alzheimer's disease by correlation- and nonlinearity-aware sparse Bayesian learning. IEEE Trans Med Imaging. 2014;33(7):1475-87.
6. Knopman DS, Amieva H, Petersen RC, Chételat G, Holtzman DM, Hyman BT, et al. Alzheimer disease. Nature reviews Disease primers. 2021;7(1):33.
7. Burns A, Iliffe S. Alzheimer's disease. BMJ. 2009;338. Available from: https://www.bmj.com/content/338/bmj.b158.
8. Bellenguez C, Küçükali F, Jansen IE, Kleineidam L, Moreno-Grau S, Amin N, et al. New insights into the genetic etiology of Alzheimer's disease and related dementias. Nature genetics. 2022;54(4):412-36.
9. Liu PP, Xie Y, Meng XY, Kang JS. History and progress of hypotheses and clinical trials for Alzheimer's disease. Signal transduction and targeted therapy. 2019;4(1):29.
10. Du X, Wang X, Geng M. Alzheimer's disease hypothesis and related therapies. Translational neurodegeneration.

2018;7(1):1-7.
11. Bao J, Wen J, Wen Z, Yang S, Cui Y, Yang Z, et al. Brain-wide genome-wide colocalization study for integrating genetics, transcriptomics and brain morphometry in Alzheimer's disease. NeuroImage. 2023:120346.
12. Wen J, Yang Z, Nasrallah IM, Cui Y, Erus G, Srinivasan D, et al. Genetic, clinical underpinnings of subtle early brain change along Alzheimer's dimensions. bioRxiv. 2022:2022-09.
13. Shen L, Thompson PM. Brain Imaging Genomics: Integrated Analysis and Machine Learning. Proceedings of the IEEE. 2020;108(1):125-62.
14. VanderWeele TJ. Mediation Analysis: A Practitioner's Guide. Annual Review of Public Health. 2016;37(1):17-32. PMID: 26653405. Available from: https://doi.org/10.1146/annurev-publhealth-032315-021402.
15. Huang YT, Pan WC. Hypothesis test of mediation effect in causal mediation model with high-dimensional continuous mediators. Biometrics. 2016;72(2):402-13.
16. Weiner MW, Veitch DP, Aisen PS, Beckett LA, Cairns NJ, Green RC, et al. The Alzheimer's Disease Neuroimaging Initiative: a review of papers published since its inception. Alzheimers Dement. 2013;9(5):e111-94.
17. Weiner MW, Veitch DP, Aisen PS, Beckett LA, Cairns NJ, Green RC, et al. Recent publications from the Alzheimer's Disease Neuroimaging Initiative: Reviewing progress toward improved AD clinical trials. Alzheimers Dement. 2017;13(4):e1-e85.
18. Saykin AJ, Shen L, Yao X, Kim S, Nho K, Risacher SL, et al. Genetic studies of quantitative MCI and AD phenotypes in ADNI: Progress, opportunities, and plans. Alzheimers Dement. 2015;11(7):792-814.
19. Shen L, Thompson PM, Potkin SG, Bertram L, Farrer LA, Foroud TM, et al. Genetic analysis of quantitative phenotypes in AD and MCI: imaging, cognition and biomarkers. Brain Imaging Behav. 2014;8(2):183-207.
20. Shen L, Kim S, Risacher SL, Nho K, Swaminathan S, West JD, et al. Whole genome association study of brain-wide imaging phenotypes for identifying quantitative trait loci in MCI and AD: A study of the ADNI cohort. Neuroimage. 2010;53(3):1051-63.
21. 1000 Genomes Project Consortium, et al. A global reference for human genetic variation. Nature. 2015;526(7571):68.
22. Das S, Forer L, Schonherr S, Sidore C, Locke AE, Kwong A, et al. Next-generation genotype imputation service and methods. Nat Genet. 2016;48(10):1284-7.
23. Wang K, Li M, Hakonarson H. ANNOVAR: functional annotation of genetic variants from high-throughput sequencing data. Nucleic acids research. 2010;38(16):e164-4.
24. Chang C, et al. Second-generation PLINK: rising to the challenge of larger and richer datasets. GigaScience. 2015;4.
25. Miller KL, Alfaro-Almagro F, Bangerter NK, Thomas DL, Yacoub E, Xu J, et al. Multimodal population brain imaging in the UK Biobank prospective epidemiological study. Nature neuroscience. 2016;19(11):1523-36.
26. Davatzikos C, Genc A, Xu D, Resnick SM. Voxel-based morphometry using the RAVENS maps: methods and validation using simulated longitudinal atrophy. NeuroImage. 2001;14(6):1361-9.
27. Ou Y, Sotiras A, Paragios N, Davatzikos C. DRAMMS: Deformable registration via attribute matching and mutual-saliency weighting. Medical image analysis. 2011;15(4):622-39.
28. Doshi J, Erus G, Ou Y, Resnick SM, Gur RC, Gur RE, et al. MUSE: MUlti-atlas region Segmentation utilizing Ensembles of registration algorithms and parameters, and locally optimal atlas selection. Neuroimage. 2016;127:186-95.
29. Chang CC, Chow CC, Tellier LC, Vattikuti S, Purcell SM, Lee JJ. Second-generation PLINK: rising to the challenge of larger and richer datasets. Gigascience. 2015;4(1):s13742-015.
30. Ibrahim I, Horacek J, Bartos A, Hajek M, Ripova D, Brunovsky M, et al. Combination of voxel based morphometry and diffusion tensor imaging in patients with Alzheimer's disease. Neuroendocrinol Lett. 2009;30(1):39-45.
31. Armstrong RA. Alzheimer's disease and the eye. Journal of Optometry. 2009;2(3):103-11.
32. Corriveau-Lecavalier N, Duchesne S, Gauthier S, Hudon C, Kergoat MJ, Mellah S, et al. A quadratic function of activation in individuals at risk of Alzheimer's disease. Alzheimer's & Dementia: Diagnosis, Assessment & Disease Monitoring. 2020;12(1):e12139.